MOLECULAR AND CELLULAR BIOLOGY, Mar. 2002, p. 1438–1445 Vol. 22, No. 5
0270-7306/02/$04.00+0 DOI: 10.1128/MCB.22.5.1438–1445.2002

Ultrastructural Cartilage Abnormalities in MIA/CD-RAP-Deficient Mice

Markus Moser,[1] Anja-Katrin Bosserhoff,[1] Ernst B. Hunziker,[2] Linda Sandell,[3] Reinhard Fässler,[4] and Reinhard Buettner[5]*

Institute of Pathology, University Hospital RWTH, D-52074 Aachen,[1] and Institute of Pathology, University of Bonn, D-53127 Bonn,[5] Germany; M. E. Müller-Institut for Biomechanics, University of Bern, CH-010 Bern, Switzerland[2]; Department of Orthopaedic Surgery, Washington University School of Medicine, St. Louis, Missouri 63110[3]; and Department of Experimental Pathology, Lund University, S-22185 Lund, Sweden[4]

Received 31 July 2001/Returned for modification 31 August 2001/Accepted 19 November 2001

MIA/CD-RAP is a small, soluble protein secreted from malignant melanoma cells and from chondrocytes. Recent evidence has identified MIA/CD-RAP as the prototype of a small family of extracellular proteins adopting an SH3 domain-like fold. It is thought that interaction between MIA/CD-RAP and specific epitopes in extracellular matrix proteins regulates the attachment of tumor cells and chondrocytes. In order to study the consequences of MIA/CD-RAP deficiency in vivo, we generated mice with a targeted gene disruption. The complete absence of MIA/CD-RAP mRNA and protein expression was demonstrated by reverse transcriptase, Western blot analysis, and enzyme-linked immunosorbent assay measurements of whole-embryo extracts. MIA$^{-/-}$ mice were viable and developed normally, and histological examination of the organs by means of light microscopy revealed no major abnormalities. In contrast, electron microscopic studies of cartilage composition revealed subtle defects in collagen fiber density, diameter, and arrangement, as well as changes in the number and morphology of chondrocytic microvilli. Taken together, our data indicate that MIA/CD-RAP is essentially required for formation of the highly ordered ultrastructural fiber architecture in cartilage and may have a role in regulating chondrocyte matrix interactions.

MIA/CD-RAP (melanoma-inhibiting activity/cartilage-derived retinoic acid-sensitive protein) was cloned as a secreted protein from human melanoma cell lines (1, 23) and independently by differential display comparing differentiated and dedifferentiated chondrocytes (8). MIA/CD-RAP is secreted from malignant melanomas and chondrosarcomas and expressed in many adenocarcinomas, including those responsible for colorectal and breast cancers (3–5). Recent evidence indicates an important role in tumor progression and metastasis, since MIA/CD-RAP mediates the detachment of melanoma cells from extracellular matrix molecules such as fibronectin (22). MIA expression levels closely parallel the capability of melanoma cells to form metastases in syngeneic animals (6, 11), and increased levels in serum have been used as a reliable and clinically useful marker to detect and monitor metastatic disease in patients with malignant melanomas (3, 20).

Recently, the three-dimensional structure of MIA/CD-RAP has been determined by multidimensional nuclear magnetic resonance spectroscopy (22) and determined independently by X-ray crystallography (14). The corresponding data indicate that MIA/CD-RAP defines a novel family of secreted proteins which adopt an SH3 domain-like fold in solution. Furthermore, nuclear magnetic resonance spectra revealed that MIA interacts with peptides matching type III human fibronectin repeats which are closely related to α4β1 integrin binding sites (22). These data support a model in which MIA/CD-RAP regulates attachment to specific components of the extracellular matrix.

In nonneoplastic tissues, MIA/CD-RAP expression is activated at the beginning of chondrogenesis throughout cartilage development (4, 8), and in vitro, it is a specific marker for chondroid differentiation. Cartilage damage due to rheumatoid arthritis releases MIA/CD-RAP from the chondroid matrix and can be monitored clinically by enhanced MIA/CD-RAP in serum (17). Based on its highly restricted activity (2), the MIA/CD-RAP promoter was used to study transcriptional mechanisms mediating chondrocyte differentiation. A 2,251-bp fragment of the murine MIA/CD-RAP 5′-end-flanking sequence contains all known functionally important trancriptional regulatory elements, including melanoma-associated transcription factor (10), AP-2, and Sox9 binding sites (19, 25, 26), and was sufficient to confer tissue-specific expression in vivo. Expression of a LacZ reporter under the control of the 2,251-bp MIA/CD-RAP promoter was observed exclusively in cartilage and transiently in embryonic mammary buds (27). These data suggested that MIA/CD-RAP may be functionally important for cartilage differentiation and for specific morphogenetic events during embryogenesis involving invasive growth.

To study the consequences of MIA/CD-RAP deficiency in vivo, we inactivated the gene by targeted germline mutation. Data described in this study indicate that MIA/CD-RAP function is required for the highly ordered fibrillar ultrastructure of cartilage but may be redundant in other tissues.

* Corresponding author. Mailing address: Institut für Pathologie, Universitätsklinikum Bonn, Sigmund-Freud-Str. 25, D-53127 Bonn, Germany. Phone: (49) 228-287-5377. Fax: (49) 228-287-5030. E-mail: Reinhard.Buettner@ukb.uni-bonn.de.

MATERIALS AND METHODS

Construction of the MIA-targeting vector and generation of gene-disrupted mice. A murine 129Sv genomic DNA library in lambda FixII was screened with a MIA cDNA probe, and two phages were isolated. A 10-kb fragment of one

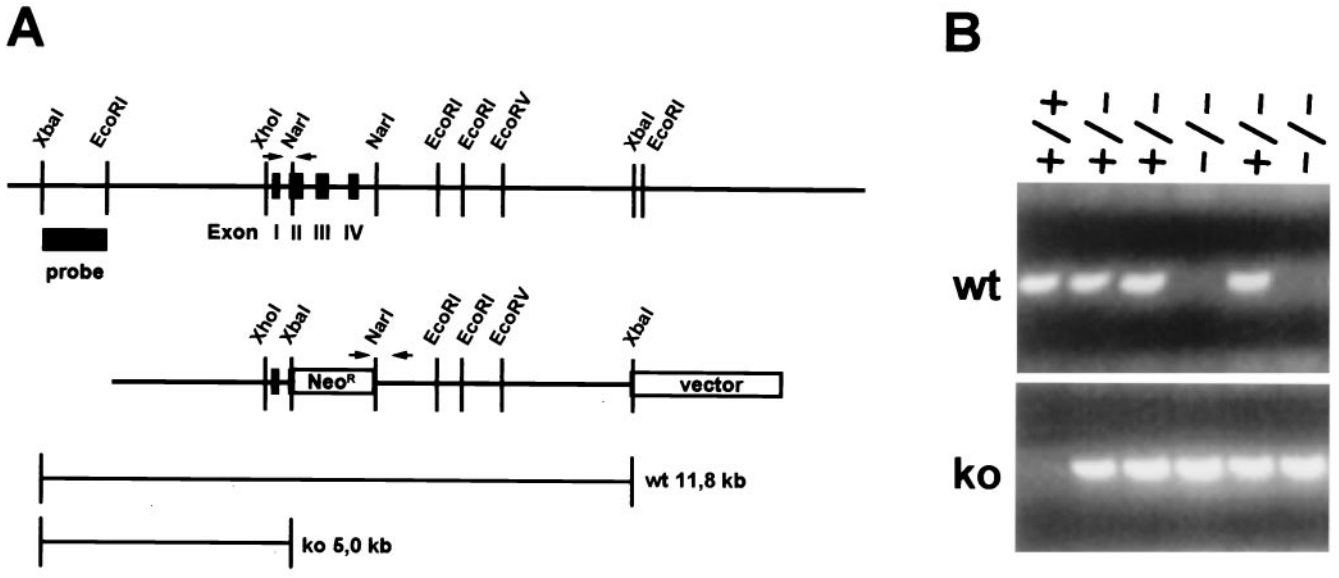

FIG. 1. MIA/CD-RAP targeting vector and genotyping of mutant mice. (A) Schematic representation of the MIA gene locus and the targeting construct. Boxes indicate exons 1 to 4 and the probe used for Southern hybridization of the neomycin-resistant stem cell clones, which recognizes the 11.8-kb wild-type and the 5-kb mutant *Xba*I fragment. (B) PCR analysis of tail biopsy DNAs from the progeny of mating heterozygotes. The positions of primer pairs for amplification of the wild-type and mutant PCR fragments are shown in panel A. wt, wild type; ko, knockout.

phage insert contained all four MIA exons and was subcloned into pBluescript. The C-terminal half of exon 2 and all of exons 3 and 4 were deleted by replacing a 1.7-kb *Nar*I fragment with a PGK-neo selection cassette. The plasmid was linearized with *Not*I and electroporated into R1 embryonic stem cells. Transfection and culture conditions have been described previously (16). Briefly, embryonic stem cells were cultured on irradiated mouse embryonic fibroblasts in the presence of 1,000 U of leukemia inhibitory factor (Gibco BRL)/ml and selected with 400 μg of G418 (Gibco BRL)/ml. A total of 240 neomycin-resistant clones were picked, expanded, and analyzed from genomic *Xba*I-digested DNA by Southern blotting. An external probe comprising a 1.3-kb genomic *Xba*I-*Eco*RI fragment of the MIA gene locus was used to identify the 11.8-kb wild-type allele and the 5-kb mutated allele.

For routine genotyping of the MIA breeding pairs, genomic-tail DNA was prepared and analyzed by PCR. The primer pair to amplify the wild-type allele was MIA-wt sense (5′-ATC CTA TCT CCA TGG CTG TGG-3′) and MIA-wt anti (5′-GCC ACT TTT GAT GGT TTG CTG G-3′). The primer pair to amplify the targeted allele was MIA-ko anti (5′-CCC ATC AGC CTC ACC GTA GGT-3′) and PGK-polyA down (5′-CGT CTC TTT ACT GAA GGC TCT TT-3′).

Cell culture. Chondrocytes were isolated from the sternums of heterozygous and MIA-deficient mice by digestion with hyaluronidase, collagenase, and DNase. Cells were cultivated in Dulbecco modified Eagle medium (DMEM) supplemented with penicillin (100 U/ml), streptomycin (10 μg/ml) (Sigma, Deisenhofen, Germany), and 10% fetal calf serum (Gibco BRL) in a humified atmosphere of 5% CO_2 at 37°C and split 1:2 at 80% confluence. To induce redifferentiation, cells were treated with transforming growth factor β for 4 days.

RNA isolation and RT-PCR. For reverse transcription-PCR (RT-PCR), total cellular RNA was isolated from three cryosections of each embryo (100 μm) or from cultivated chondrocytes with an RNeasy kit (Qiagen, Hilden, Germany). The integrity of the RNA preparations was controlled on a 1% agarose-formaldehyde gel. The reverse transcriptase reaction was performed in a 20-μl reaction volume containing 2 μg of total cellular RNA, 4 μl of 5× first-strand buffer (Gibco BRL), 2 μl of 0.1 M dithiothreitol, 1 μl of the dN_6 primer (10 mM), 1 μl of the deoxynucleoside triphosphates (10 mM), and diethyl pyrocarbonate-water. The reaction mix was incubated for 10 min at 70°C. Then, 1 μl of Superscript II reverse transcriptase (Gibco BRL) was added and RNAs were transcribed for 1 h at 37°C. Subsequently, reverse transcriptase was inactivated at 70°C for 10 min and RNA was degraded by digestion with 1 μl of RNase A (10 mg/ml) at 37°C for 30 min. cDNAs were controlled by PCR amplification of β-actin. MIA was amplified by PCR with specific primers, resulting in a 311-bp fragment (mMIA for [5′-CTG GCT GAC CGG AAG CTG TG-3′] and mMIA rev [5′-GCT ACT GGG GAA ATA GCC C-5′]). Next, TANGO, OTOR, MIA2, and type I and II collagens were amplified. PCRs were performed in a 100-μl reaction volume containing 1 μl of cDNA, 10 μl of 10× PCR buffer, 1 μl of the deoxynucleoside triphosphates, 1 μl of each primer, and 1 μl of *Taq* polymerase (Roche, Mannheim, Germany). The amplification reactions were performed with 30 repetitive cycles of denaturing for 1 min at 94°C and annealing for 1 min at 58°C and a final extension step at 72°C for 1.5 min. The PCR products were resolved on 1.8% agarose gels.

ISH. In situ hybridization (ISH) to paraffin-embedded mouse hindlimbs on day 1 postnatalis (p.n.) was performed as described previously (15) using ^{33}P-labeled sense and antisense cRNA riboprobes (4). Briefly, proteinase K-pretreated slides (10 μg/ml) were acetylated in acetic anhydride diluted 1:400 in 0.1 M triethanolamine (pH 8) and hybridized overnight in 50% formamide–10% dextran sulfate–10 mM Tris (pH 8)–10 mM NaP_i (pH 7)–2× SSC (1× SSC is 0.15 M NaCl plus 0.015 M sodium citrate)–5 mM EDTA (pH 8)–150 μg of tRNA/ml–10 mM dithiothreitol–10 mM β-mercaptoethanol supplemented with 5×10^4 cpm of ^{33}P-labeled sense or antisense riboprobes/μl at 50°C. Finally, slides were washed twice in 50% formamide–2× SSC–20 mM β-mercaptoethanol, digested with RNase A (20 μg/ml) for 30 min at 37°C, and then washed again three times with the same washing buffer for 30 min each at 50°C. Following dehydration, slides were coated with Kodak (Rochester, N.Y.) NTB2 emulsion and exposed for 8 to 10 days.

Skeletal staining. Skeletal staining of whole mouse embryos was performed 15.5 days postcoitum as described previously (24). In brief, whole embryos were fixed for 5 days in 95% ethanol and transferred to acetone for 2 days. Staining was performed with 0.005% alzarin red S–0.015% alcian blue 8GS–5% acetic acid–90% ethanol for 3 days at 37°C. Samples were washed in H_2O and cleared for 2 days in 1% KOH, followed by clearing steps in 0.8% KOH–20% glycerol, in 0.5% KOH–50% glycerol, and in 0.2% KOH–80% glycerol for 1 week each. Cleared skeletons were stored in 100% glycerol and photographed.

Western blots. Three cryosections of each embryo (100 μm) were lysed in 200 μl of radioimmunoprecipitation assay buffer (Roche), and protein concentrations were determined using the bicinchoninic acid protein assay reagent (Pierce, Bonn, Germany). Twenty micrograms of protein per lane was denatured at 94°C for 10 min after the addition of Roti load buffer (Roth, Karlsruhe, Germany) and subsequently separated on 4 to 20%-gradient sodium dodecyl sulfate-polyacrylamide electrophoresis gels. After we transferred the proteins by Western blotting onto polyvinylidene difluoride membranes (Bio-Rad, Richmond, Calif.), the membranes were blocked in 3% bovine serum albumin–phosphate-buffered saline for 1 h and incubated with a 1:30 dilution of primary polyclonal anti-MIA antibody overnight at 4°C. A 1:300 dilution of rabbit anti-immunoglobulin G

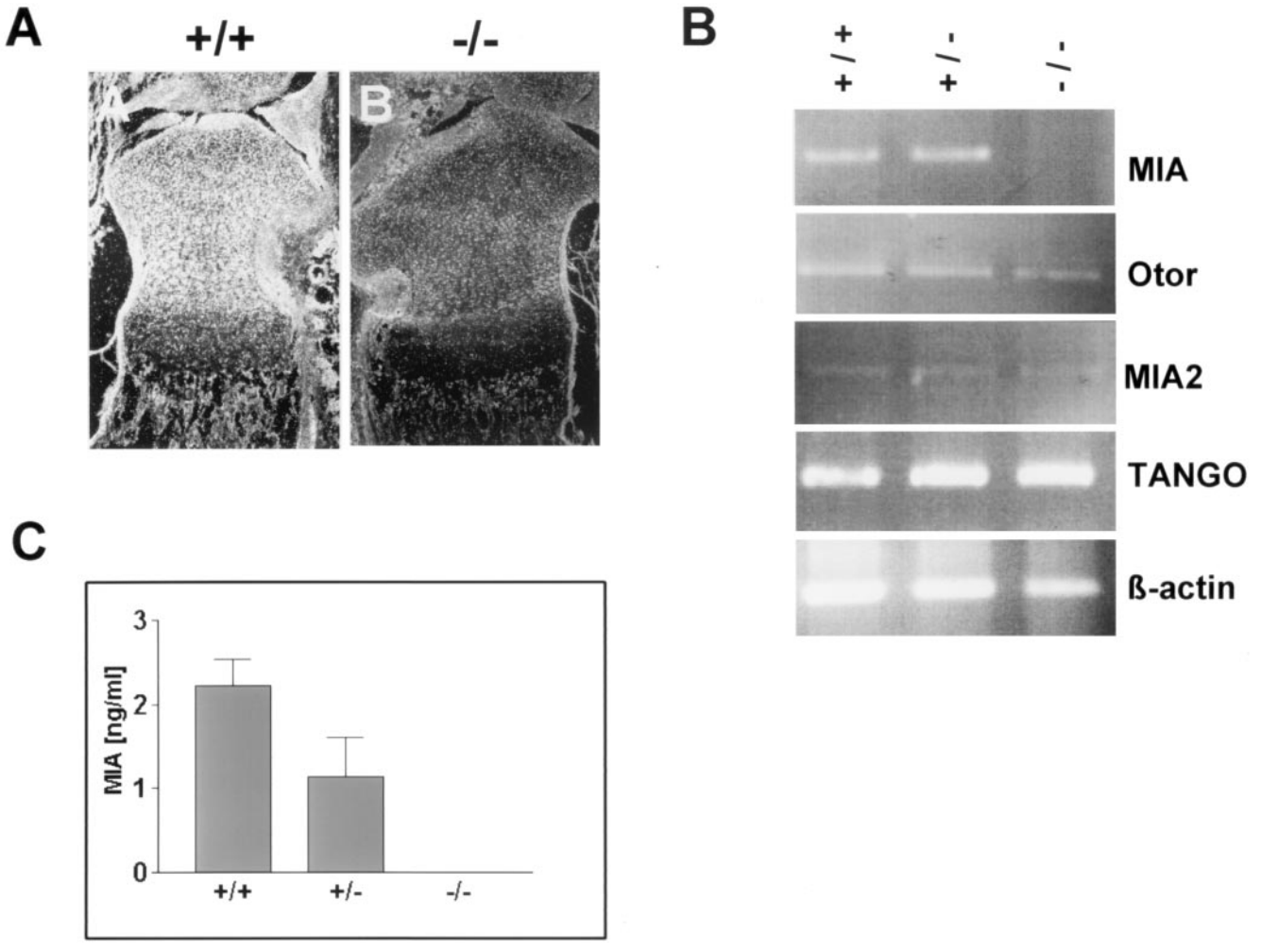

FIG. 2. MIA/CD-RAP mRNA and protein expression in wild-type and mutant mice. (A) ISH of tibia head sections at day 1 p.n. (B) RT-PCR using MIA/CD-RAP-specific, OTOR-specific, TANGO-specific, MIA2-specific, and β-actin-specific primer pairs from prenatal mice at E18.5; (C) measurement of soluble MIA/CD-RAP extracted from E18.5 embryos by a quantitative ELISA.

coupled to alkaline phosphatase (Roche) was used as secondary antibody. Staining was performed with BCIP (5-bromo-4-chloro-indolylphosphate)-nitroblue tetrazolium tablets (Sigma).

MIA ELISA. MIA expression was measured by a one-step enzyme-linked immunosorbent assay (ELISA) of the lysates of the mouse embryos. Two monoclonal antibodies (MAbs) directed against 14-meric N-terminal and C-terminal peptides (MAb 1A12 and MAb 2F7; Roche) were raised and conjugated to horseradish peroxidase and biotin, respectively. Twenty microliters of lysate was coincubated with biotinylated MAb 2F7 and horseradish peroxidase-conjugated MAb 1A12 in streptavidin-coated 96-well plates for 45 min. After the wells were washed three times with phosphate-buffered saline, 200 μl of ABTS solution (2,2′-azino-di-[3-ethylbenzthiazoline sulfonate(6)]; Roche) was incubated in the wells for 30 min and measured colorimetrically at a wavelength of 405 nm. By using standard concentrations of recombinant MIA purified from stably transfected CHO cells, we measured linear signals at MIA concentrations between 0.1 and 50 ng/ml.

Immunohistochemistry. Paraffin-embedded preparations of newborn wild-type and $MIA^{-/-}$ mice were immunostained with collagen type I- and type II-specific antibodies using the avidin-biotin complex method (LSAB2 kit; DAKO, Hamburg, Germany). The tissues were deparaffinated, rehydrated, and subsequently incubated with primary MAbs (both diluted 1:100; ICN) overnight at 4°C. The secondary antibody supplied with the kit was incubated for 30 min at room temperature. Antibody binding was visualized with 3-amino-9-ethylcarbazole solution (for the LSAB2 kit). Finally, the tissues were counterstained with hematoxylin.

Electron microscopy. The articular cartilage of the femoral and tibial portions of the knee joints of control and null mice were chemically fixed in an aqueous solution of glutaraldehyde (2.5%) in 0.1 M sodium cacodylate buffer (pH 7.4). Following fixation at room temperature over 2 days, postfixation was started with a 1% osmium tetroxide solution (sodium cacodylate buffer, pH 7.4) over a period of 4 h at room temperature and then over 20 h at 4°C. Thereafter, specimens were washed four times in isotonic sodium cacodylate buffer (0.1 M; pH 7.4) and dehydrated through a graded series of ethanol starting at 70% (vol/vol) over a total time period of 3 h. Thereafter, embedding was initiated in Epon 812 with polypropylene oxide-Epon mixtures over a period of 9 days. Polymerization was performed at 60°C over 1 week. One-micrometer semithin sections for light microscopic examination were cut with a Leica Ultracut S microtome and stained with toluidine blue 0. Thin sections were cut on the same instrument at a thickness of about 60 nm and stained with uranyl acetate and lead citrate according to standard protocols (12, 13).

Pericellular-territorial and interterritorial matrix compartments were analyzed separately. Matrix compartments were defined as described previously (9).

RESULTS

Previously, we isolated genomic clones from the mouse strain 129Sv and provided a detailed characterization of the murine genomic structure (4). The gene encompasses four exons that are 229, 134, 111, and 88 bp in length and codes for an export signal and a mature polypeptide of 107 amino acids. We used

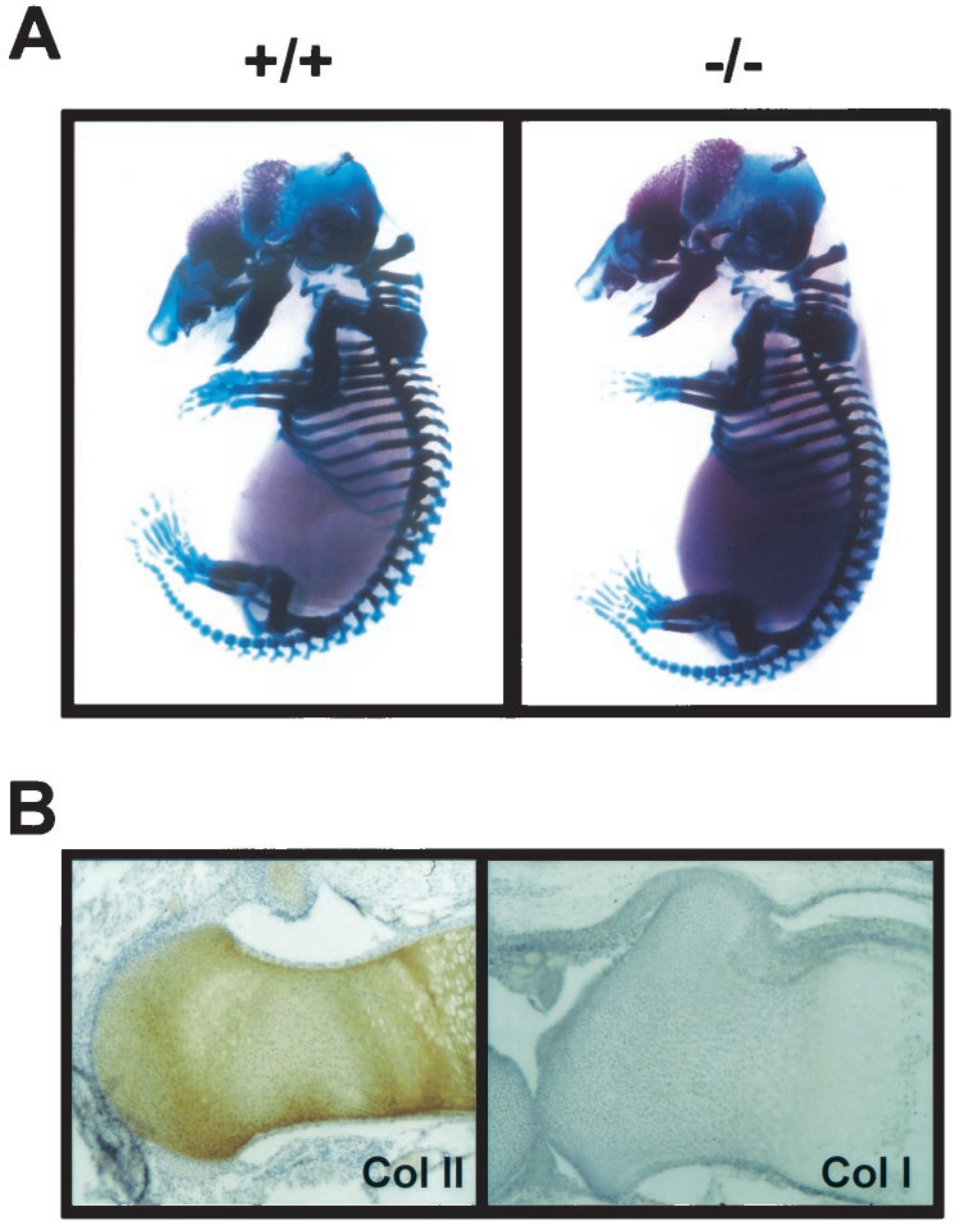

FIG. 3. Gross morphology of the skeletal system and hyaline joint cartilage in MIA/CD-RAP$^{-/-}$ mice. (A) Skeletal preparations of E15.5 mouse embryos; (B) immunohistochemical stainings of collagens I and II (Col I and II) in MIA-deficient hyaline cartilage.

*Nar*I sites within exon 2 and downstream from exon 4 to replace a large portion of the gene by a *neo* selection cassette (Fig. 1A). As a result, the mutated MIA allele codes for a small, N-terminally truncated polypeptide of only 57 amino acid residues. Based on our previous determination of the three-dimensional structure in solution, this truncation leads to inactivation of the protein, as structurally required β sheets of the SH3 fold and an essential disulfide bond required for protein stabilization in solution are disrupted (22). Genotyping of neomycin-resistant stem cell clones was performed by Southern blotting with a genomic probe hybridizing to the 11.8-kb *Xba*I wild-type fragment and the 5-kb mutated fragment (data not shown). For routine genotyping of mouse tail DNAs, two PCRs specific for the wild-type and mutated alleles were designed. Primers are indicated schematically in Fig. 1A, and a representative gel resulting from wild-type, heterozygous, and homozygous mutant mice is shown in Fig. 1B.

MIA$^{-/-}$ mice were born at the expected Mendelian frequency, were fertile, and showed no phenotypic abnormality based on macroscopic inspection and histological examination of the internal organs by light microscopy. To verify the absence of functional MIA/CD-RAP mRNA and protein in MIA-deficient mice, we performed ISH and RT-PCR and quantitated MIA protein from whole-embryo extracts by means of an ELISA (3). Our results show the absence of MIA mRNA expression in articular cartilage of postnatal mice (Fig. 2A) and the absence of mRNA

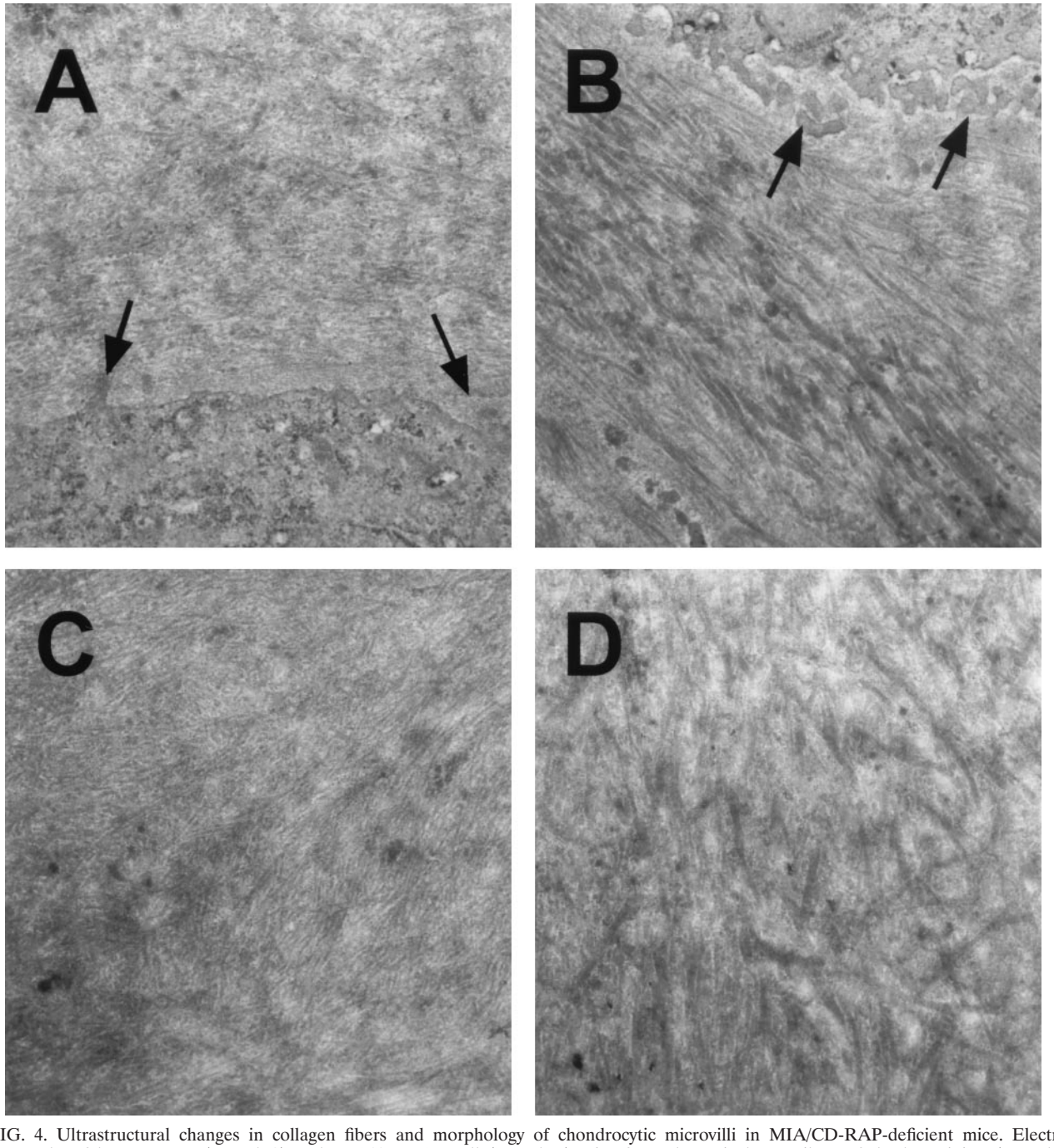

FIG. 4. Ultrastructural changes in collagen fibers and morphology of chondrocytic microvilli in MIA/CD-RAP-deficient mice. Electron micrographs of heterozygote (A and C) and MIA/CD-RAP-null (B and D) mice from the articular cartilage of the knee joint. (A and B) Pericellular-territorial matrix compartment. Arrows indicate microvilli. Shown are a homogenous distribution of fine collagen fibrils in the compartments close to the cell surface (A) and the high variation in the density of fibrils as well as in fibrillar diameters (B). The images in panels C and D are taken further away from cells in the interterritorial matrix compartments. In heterozygote mice (C), a more homogenous fine fibrillar collagen network is identifiable, whereas in knockout mice (D), the fibril diameters vary considerably in size as well as in fibrillar density and the architecture is more irregular. Magnification, ×28,900.

and protein (Fig. 2B and C) in lysates from whole embryos on embryonic day 18.5 (E18.5). We chose to analyze animals at this stage because previous data indicated that MIA/CD-RAP expression was highest during chondrogenesis of the growing skeletal system (4). In comparison, strong mRNA and protein expression was detected in wild-type embryos and intermediate protein levels were detected in heterozygous littermates. Data obtained from quantitation of MIA/CD-RAP by ELISA were confirmed by Western blotting (data not shown). Further analyses by quantitative real-time PCR indicated that the close MIA homologs OTOR/MIAL (7, 18), TANGO, and MIA2 were not upregulated in MIA-deficient embryos (Fig. 2B).

TABLE 1. Electron microscopic findings

Mice	Characteristic					
	Chondrocytes		Matrix architecture			
	Size and shape	Cell processes (microvilli)	Cytoplasma organelles	Pericellular matrix compartment	Territorial matrix compartment	Interterritorial matrix compartment
$MIA^{+/+}$ and $MIA^{+/-}$	Normal	Normal length	Normal	Low density of fine collagen fibrils	Increased normal collaginous fibrillar network	Normal parallel-oriented fine fibrillar collaginous network
$MIA^{-/-}$	Normal	Increased no., extended length	Normal	Increased collagen fibrillar density, increased fibrillar diam, larger, variation in fibril diam and size distribution, capsule-like accumulations of fibrils	Increased collagen fibrillar density, larger fibrillar diam and fibril diam variations	Larger fibrillar diam, larger cross-sectioned fibrillar area variations, higher degree of disorientation

Because specific MIA/CD-RAP expression patterns were described to occur in cartilage, melanocytic cells, and breast bud development, we analyzed these tissues in further detail. The histological morphology of breast tissue (data not shown) and the function of the lactating glands were unaffected by the mutation, since $MIA^{-/-}$ mothers were able to feed and raise their offspring normally. Also, immunohistological staining of skin biopsies recovered at day 4 p.n. with a tyrosinase-specific antibody indicated normal morphology, location, and numbers of melanocytes in the dermis. Taken together, these data suggest that MIA/CD-RAP expression is redundant or not required for normal development of mammary glands and melanoblast migration and differentiation. Recently, we observed overlapping patterns of expression of two novel homologs of the emerging MIA gene family, MIA-2 and TANGO (unpublished observations). It is therefore possible that MIA/CD-RAP function in these tissues is compensated for by the structurally related proteins MIA-2 and TANGO.

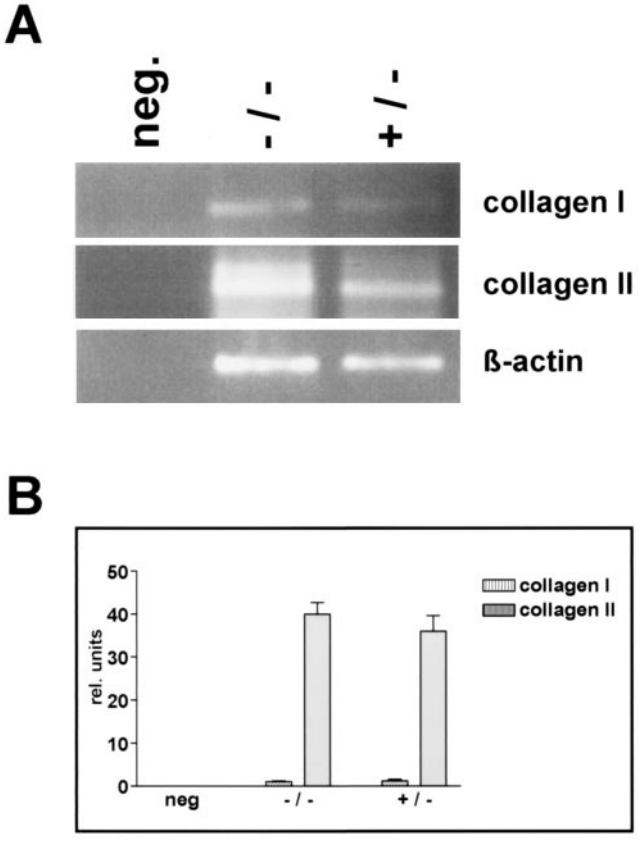

FIG. 5. Differentiation of MIA/CD-RAP-deficient chondrocytes in vitro. (A) RT-PCR using type I collagen- and type II collagen-specific primers on RNAs isolated from redifferentiated MIA/CD-RAP-deficient chondrocytes and heterozygous cells; (B) ratios of collagen I and II relative to β-actin expression. neg., negative; rel., relative.

Skeletal preparations of E15.5 wild-type and knockout animals revealed normal development and gross morphology of the skeletal system, indicating undisturbed chondrogenesis and regular enchondral and desmal ossification (Fig. 3A). In addition, light microscopic examination of histological slides stained with hematoxylin, eosin, and alcian blue and analysis of MIA/CD-RAP expression by ISH revealed no pathological alteration in hyaline or fibrous cartilage (Fig. 2A and data not shown). Immunhistochemical stainings of tibia and femur sections showed identical patterns of type II collagen distribution and the absence of type I collagen in MIA/CD-RAP-deficient and wild-type cartilage (Fig. 3B). Further expression of type X collagen and aggrecan remained unchanged in knockout mice compared to that of wild-type littermates (data not shown).

However, more detailed examination of articular cartilage obtained from knee joints of 8-month-old animals by transmission electron microscopy revealed distinct ultrastructural abnormalities in $MIA^{-/-}$ mice. Thin sections were examined in a Hitachi 7000-B electron microscope and systematically analyzed in the superficial third, the middle third, and the lower third of the articular cartilage tissue. Electron micrographs were taken at four different magnifications in order to analyze cell shapes, sizes, and cytoplasmatic organelle density. At intermediate magnifications, we assessed organelle structure as well as matrix compartment architecture, and at high magnifications, we studied the collagen fibrillar architecture in cartilage matrix compartments.

As shown by representative electron micrographs in Fig.

4, increased sizes and irregular arrangement of fibers were observed in MIA/CD-RAP-defective cartilage. In both the pericellular-territorial and interterritorial matrix compartments, we detected significant irregularities in collagen fiber density, diameter, and arrangement, as well as changes in the number and morphology of chondrocytic microvilli. A detailed overview of electron microscopic findings is summarized in Table 1.

To test the intrinsic ability of cultivated MIA/CD-RAP-deficient cells to undergo cartilaginous differentiation, dedifferentiated chondrocytes were redifferentiated in vitro by treatment with transforming growth factor β for 4 days. Redifferentiation was determined by RT-PCR for collagen type II and the absence of collagen type I expression. As illustrated in Fig. 5, no difference was observed with respect to collagen expression patterns between MIA/CD-RAP-deficient and heterozygous cells.

DISCUSSION

Recent studies of MIA/CD-RAP indicate that the protein adopts an SH3 domain-like fold in solution and is secreted from melanoma cells to modify attachment to extracellular matrix molecules (14, 21, 22). Although MIA/CD-RAP expression closely parallels chondrocytic differentiation both in vivo and in vitro, its function in cartilage remains unclear. Here, we provide the first evidence that a nonredundant MIA/CD-RAP function is required for the highly ordered ultrastructural fiber architecture in hyaline joint cartilage. In addition, we observed changes in the number and morphology of chondrocytic microvilli, suggesting alterations in cell-matrix interactions. Therefore, we speculate that specific interactions between the MIA/CD-RAP SH3 domain-like fold and cartilage matrix molecules contribute to the organization of the cartilaginous ultrastructure but are not required to trigger the differentiation program in vitro. Because we did not detect any obvious matrix degeneration in the articular cartilage even of older mice at the age of 18 months, further studies after enhanced mechanical stress exposure will be required to investigate whether the architectural defects observed in MIA knockout mice predispose them to osteoarthritis.

Very recently we detected that MIA/CD-RAP belongs to a family of four homologous and evolutionarily conserved proteins, MIA/CD-RAP, OTOR/MIAL (7, 18), MIA-2, and TANGO (Bosserhoff et al., submitted), which are expressed in numerous different tissues. Since all four proteins are structurally conserved SH3 domain-like proteins, it can be assumed that, like MIA/CD-RAP, these proteins are soluble in serum and are widely distributed in the organism. Further analyses of the phenotypes of mice with double, triple, and quadruple defects will be required to assess whether partial redundancy between these genes exists.

ACKNOWLEDGMENTS

We thank Sandra Dahmen, Judith Dahmen, Ellen Paggen, Astrid Hamm, and Nicole Krott for excellent technical assistance.

This work was supported by grants from the Swedish Medical Research Council to R.F. and from the Deutsche Forschungsgemeinschaft and the Deutsche Krebshilfe to R.B. and A.-K.B.

REFERENCES

1. **Blesch, A., A. K. Bosserhoff, R. Apfel, C. Behl, B. Hessdoerfer, A. Schmitt, P. Jachimczak, F. Lottspeich, R. Buettner, and U. Bogdahn.** 1994. Cloning of a novel malignant melanoma-derived growth regulatory protein. Cancer Res. **54:**5695–5701.
2. **Bosserhoff, A. K., R. Hein, U. Bogdahn, and R. Buettner.** 1996. Structure and promoter analysis of the gene encoding the human melanoma-inhibiting protein. J. Biol. Chem. **271:**490–495.
3. **Bosserhoff, A. K., M. Kaufmann, B. Kaluza, I. Bartke, H. Zirngibl, R. Hein, W. Stolz, and R. Buettner.** 1997. Melanoma-inhibiting activity, a novel serum marker for progression of malignant melanoma. Cancer Res. **57:**3149–3153.
4. **Bosserhoff, A. K., S. Kondo, M. Moser, U. Dietz, N. G. Copeland, D. J. Gilbert, N. A. Jenkins, R. Buettner, and L. J. Sandell.** 1997. The mouse MIA/CD-RAP gene: structure, chromosomal localization and expression in cartilage and chondrosarcoma. Dev. Dyn. **208:**516–525.
5. **Bosserhoff, A. K., M. Moser, R. Hein, M. Landthaler, and R. Buettner.** 1999. In situ expression patterns of melanoma-inhibiting activity (MIA) in melanomas and breast cancers. J. Pathol. **187:**446–454.
6. **Bosserhoff, A. K., B. Echtenacher, R. Hein, and R. Buettner.** 2001. Functional role of MIA in regulating invasion and metastasis of malignant melanoma cells in vivo. Melanoma Res. **11:**417–421.
7. **Cohen-Salmon, M., D. Frenz, W. Liu, E. Verpy, S. Voegeling, and C. Petit.** 2000. Fdp, a new fibrocyte-derived protein related to MIA/CD-RAP, has an in vitro effect on the early differentiation of the inner ear mesenchyme. J. Biol. Chem. **275:**40036–40041.
8. **Dietz, U., and L. J. Sandell.** 1996. Cloning of a retinoic acid-sensitive mRNA expressed in cartilage and during chondrogenesis. J. Biol. Chem. **271:**3311–3316.
9. **Eggli, P. S., W. Herrmann, E. B. Hunziker, and R. K. Schenk.** 1985. Matrix compartments in the growth plate of the proximal tibia of rats. Anat. Rec. **211:**246–257.
10. **Golob, M., R. Buettner, and A. K. Bosserhoff.** 2000. Characterization of a transcription factor binding site, specifically activating MIA transcription in melanoma. J. Investig. Dermatol. **115:**42–47.
11. **Guba, M., A. K. Bosserhoff, M. Steinbauer, C. Abels, M. Anthuber, R. Buettner, and K. W. Jauch.** 2000. Overexpression of melanoma inhibitory activity (MIA) enhances extravasation and metastasis of A-mel 3 melanoma cells in vivo. Br. J. Cancer **83:**1216–1222.
12. **Hunziker, E. B., J. Wagner, and D. Studer.** 1996. Vitrified articular cartilage reveals novel ultra-structural features respecting extracellular matrix architecture. Histochem. Cell Biol. **106:**375–382.
13. **Hunziker, E. B., M. Nichel, and D. Studer.** 1997. Ultrastructure of adult human articular cartilage matrix after cryotechnical processing. Microsc. Res. Tech. **37:**271–284.
14. **Lougheed, J. C., J. M. Holton, T. Alber, J. F. Bazan, and T. M. Handel.** 2001. Structure of melanoma inhibitory activity protein, a member of a recently identified family of secreted proteins. Proc. Natl. Acad. Sci. USA **98:**5515–5520.
15. **Moser, M., A. Pscherer, A. Imhof, R. Bauer, W. Amselgruber, F. Sinowatz, F. Hofstaedter, R. Schule, and R. Buettner.** 1995. Molecular cloning and characterization of a second AP-2 transcription activator gene, AP-2β. Development **121:**2779–2788.
16. **Moser, M., A. Pscherer, C. Roth, J. Becker, G. Mücher, K. Zerres, C. Dixkens, J. Weis, L. Guay-Woodford, R. Buettner, and R. Fässler.** 1997. Enhanced apoptotic cell death of renal epithelial cells in mice lacking transcription factor AP-2β. Genes Dev. **11:**1938–1948.
17. **Müller-Ladner, U., A. K. Bosserhoff, K. Dreher, R. Hein, M. Neidhart, S. Gay, J. Schoelmerich, R. Buettner, and B. Lang.** 1999. MIA (melanoma inhibitory activity): a potential serum marker for rheumatoid arthritis. Rheumatology **38:**148–154.
18. **Robertson, N. G., S. Heller, J. S. Lin, B. L. Resendes, S. Weremowicz, C. S. Denis, A. M. Bell, A. J. Hudspeth, and C. C. Morton.** 2000. A novel conserved cochlear gene, OTOR: identification, expression analysis, and chromosomal mapping. Genomics **66:**242–248.
19. **Sakano, S., Y. Zhu, and L. J. Sandell.** 1999. Cartilage-derived retinoic acid-sensitive protein and type II collagen expression during fracture healing are potential targets for Sox9 regulation. J. Bone Miner. Res. **14:**1891–1901.
20. **Stahlecker, J., A. Gauger, A. Bosserhoff, R. Buttner, J. Ring, and R. Hein.** 2000. MIA as a reliable tumor marker in the serum of patients with malignant melanoma. Anticancer Res. **20:**5041–5044.
21. **Stoll, R., C. Renner, D. Ambrosius, M. Golob, W. Voelter, R. Buettner, A. K. Bosserhoff, and T. A. Holak.** 2000. Sequence-specific 1H, 13C, and 15N assignment of the human melanoma inhibitory activity (MIA) protein. J. Biomol. NMR **17:**87–88.
22. **Stoll, R., C. Renner, M. Zweckstetter, M. Brüggert, D. Ambrosius, S. Palme, R. A. Engh, M. Golob, I. Breibach, R. Buettner, W. Voelter, T. A. Holak, and A. K. Bosserhoff.** 2001. The extracellular human melanoma inhibitory activity (MIA) protein adopts an SH3 domain-like fold. EMBO J. **20:**340–349.
23. **van Groningen, J. J., H. P. Bloemers, and G. W. Swart.** 1995. Identification of melanoma inhibitory activity and other differentially expressed messenger RNAs in human melanoma cell lines with different metastatic capacity by messenger RNA differential display. Cancer Res. **55:**6237–6243.

24. **Wallin J., J. Wilting, H. Koseki, R. Fritsch, B. Christ, and R. Balling.** 1994. The role of Pax-1 in axial skeleton development. Development **120:**1109–1121.
25. **Xie, W. F., S. Kondo, and L. J. Sandell.** 1998. Regulation of the mouse cartilage-derived retinoic acid-sensitive protein gene by the transcription factor AP-2. J. Biol. Chem. **273:**5026–5032.
26. **Xie, W. F., X. Zhang, S. Sakano, V. Lefebvre, and L. J. Sandell.** 1999. Trans-activation of the mouse cartilage-derived retinoic acid-sensitive protein by Sox9. J. Bone Miner. Res. **14:**757–763.
27. **Xie, W. F., X. Zhang, and L. J. Sandell.** 2000. The 2.2-kb promoter of cartilage-derived retinoic acid-sensitive protein controls gene expression in cartilage and embryonic mammary buds of transgenic mice. Matrix Biol. **19:**501–509.